Experimental Investigations of the Compressible Turbulent Boundary Layer at Very High Reynolds Numbers

D. R. Moore* and J. Harkness†
Ling-Temco-Vought, Inc., Dallas, Texas

The present experimental program was undertaken with the objective of extending the Reynolds number range of available experimental skin-friction data to approximately 10^9. Included in this paper are the results of two series of tests in which local surface shear stress and boundary-layer velocity profile measurements were made on aerodynamically smooth isobaric, adiabatic surfaces. The tests were conducted in the LTV High-Speed Wind Tunnel at a nominal Mach number of 2.8. In the first series, a 10-ft-long flat-plate model served as the test surface. In the second series, the floor of the tunnel supersonic diffuser, modified to provide an effective extension of the tunnel test section, was the test surface. The paper contains a description of the test apparatus and procedures as well as a discussion of the results. The program objective was accomplished in that a Reynolds number range of $2.32 \times 10^7 \leqq R_x \leqq 1.41 \times 10^9$ was covered. These results represent a significant extension of the Reynolds number range of available experimental skin-friction data.

Nomenclature

C_f = local skin-friction coefficient
M = Mach number
P = pressure
P_{t_2} = total pressure behind a normal shock
q = dynamic pressure
R_x = Reynolds number based on $x - \rho_1 U_1 x/\mu_1$
R_θ = Reynolds number based on $\theta - \rho_1 U_1 \theta/\mu_1$
R = gas constant
T = absolute temperature
U = velocity
U_τ = friction velocity $- (\tau_w/\rho_w)^{1/2}$
x = distance along test surface in direction of flow
y = coordinate distance normal to the test surface
γ = specific heat ratio
δ = boundary-layer thickness
δ^* = displacement thickness
η = law of the wall dimensionless spatial coordinate $- \rho_w U_\tau y/\mu_w$
θ = boundary-layer momentum thickness [Eq. (11)]
μ = viscosity
ρ = mass density
σ = compressibility factor $- \{[(\gamma - 1)/2]M_1^2\}\{1 + [(\gamma - 1)/2]M_1^2\}^{-1}$
τ = shearing stress
ϕ = dimensionless velocity $- U/U_\tau$
ϕ^* = dimensionless velocity corrected for compressibility

Subscripts

0 = isentropic stagnation conditions
1 = local conditions at the outer edge of the boundary layer
w = wall conditions

I. Introduction

THE accurate prediction of the skin-friction drag forces acting on vehicles in high-speed atmospheric flight has for many years been an important design consideration. Recent vehicular concepts have greatly increased the importance of this prediction capability, since for some highly streamlined configurations the skin-friction drag can be as much as 50% of the total drag. These designs also have introduced flight conditions such that portions of the vehicles may experience very high Reynolds number flows. The calculation methods used for the prediction of skin-friction drag forces for turbulent boundary-layer flows are generally based on empirical or semiempirical analyses. The experimental data available for the formulation and validation of these methods have been restricted to flows of Reynolds numbers less than 10^8, and the extrapolation of such methods for higher Reynolds numbers introduces a certain degree of uncertainty.

The investigation reported herein was undertaken with the purpose of extending the Reynolds number range of available experimental skin-friction data to approximately 10^9. The over-all program was divided into three test phases. Reported herein are the results of the first two phases involving skin-friction and boundary-layer total pressure distribution measurements on aerodynamically smooth, isobaric and adiabatic surfaces. The third test phase, which is yet to be accomplished, will involve the investigation of the effects of uniform grain-type roughness on local skin friction at high Reynolds numbers. The third phase will also include drag measurements on forward- and aft-facing steps in high Reynolds number flows. The ratio of step height to boundary-layer thickness will vary from approximately 0.025 to 0.10. All tests are at a Mach number of 2.80.

In order to obtain the desired high Reynolds number flows it was decided to use the floor of the LTV High-Speed Wind Tunnel supersonic diffuser as the test surface. An effective extension of the tunnel test section was provided by opening the diffuser and making certain fairing modifications to the upper and lower walls. A feasibility test was conducted to determine the static pressure distribution along the open diffuser without the fairing modifications. Only a slight adverse pressure gradient was found and the range of operating pressures was determined. The vibrational loads and frequencies of the diffuser structure were also measured during this feasibility test.

Standard experimental techniques were used in obtaining the boundary-layer measurements. The local shear stresses were measured with a floating-element-type balance having the same basic design used in several previous studies. The total pressure surveys, which were used to determine the boundary-layer velocity distribution, were obtained by impact probes traversing the boundary layer. In the first test phase a 10-ft-long smooth flat-plate model mounted in the

Presented as Preprint 64-592 at the AIAA Transport Aircraft Design and Operations Meeting, Seattle, Wash., August 10–12, 1964; revision received November 30, 1964. Work sponsored by the U. S. Air Force Aeronautical Systems Division under its New Advanced Systems Program Office.

* Research Scientist, LTV Research Center. Member AIAA.
† Senior Scientist, LTV Research Center. Member AIAA.

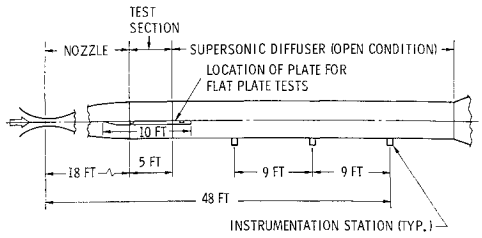

Fig. 1 Schematic drawing of wind-tunnel configuration for skin-friction tests.

tunnel test section served as the test surface. The flat-plate tests not only provided an extension of the Reynolds number range of available experimental skin-friction data, but provided control data for the second phase tests using the floor of the diffuser as the test surface. Figure 1 presents a sketch of the flat-plate model and diffuser installations.

The major objection to measuring skin friction on the floor of a wind tunnel is that the dimension x from the origin of the boundary layer to the test station is unknown. This difficulty was overcome by determining the momentum thickness θ from the total pressure survey data across the boundary layer. A relationship was derived relating θ to x by integration of the zero pressure gradient momentum equation $C_f = 2\ d\theta/dx$, with the constant of integration evaluated from the flat-plate test data, for which both θ and x were known. The derivation of this expression is discussed in the data reduction section of this paper. This paper also contains descriptions of the experimental apparatus and test procedures, and a discussion of the results obtained.

II. Experimental Apparatus and Test Procedure

The wind-tunnel facility, the skin-friction balance, and the total pressure survey drive mechanism were common to both phases of the test program. In general, the test procedures were the same for both the flat-plate and diffuser floor tests. The following paragraphs in this section of the report describe briefly the apparatus and procedures used in these tests.

A. Wind Tunnel

The LTV High-Speed Wind Tunnel, which has been described in detail in Ref. 1, is a blow-down, variable Mach number tunnel exhausting to the atmosphere. The tunnel has the capability of both transonic and supersonic testing by utilizing interchangeable 4- × 4-ft test sections. Storage air at a maximum pressure of 600 psia and a nominal temperature of 100°F is held in six tanks having a total volume of 28,000 ft³. Tunnel running times under the conditions of the present tests vary with tunnel stilling chamber pressure from approximately 10 to 30 sec of stabilized flow.

The electronic data recording system associated with the wind-tunnel records the data on magnetic tape during the run and later punches data cards. These cards are used in IBM 7090 routines to reduce the data to the desired form. For the present tests the data were sampled 20 times/sec.

B. Skin-Friction Balance

The basic design of the skin-friction balance used in the present tests is typical of those used in several previous experiments for the measurement of local surface shear stress. This floating-element-type balance is shown schematically in Fig. 2. The 2-in.-diam floating element was supported by two sets of stainless-steel flexures, which were rigidly attached to the balance frame. The total gap (difference in diameters) between the floating element and the balance case was 0.014 in., and the element was positioned to allow a 0.010-in. deflection in the streamwise direction. Deflection of the flexures resulting from shear forces acting on the surface element is reflected by the output voltage of the Schaevitz linear differential transformer. The transformer coil is mounted in the balance frame and the core is fixed with respect to the moving element. A device was constructed by which a shear force vs output voltage calibration of the balance could be readily obtained. One set of flexures was used which permitted the force range of the entire test program to be covered. The balance calibrations were made before each run using the wind-tunnel data system.

The accelerometer data obtained in the feasibility test indicated that the balance would be subjected to vibrations which might affect its performance. A viscous damping provision, therefore, was included in the design as may be observed in Fig. 2. A silicone grease was used as the damping fluid.

Prior to tunnel installation, the balance and associated equipment underwent numerous check calibrations. It was determined from these bench tests that balance calibration curves were consistent and linear within $\frac{1}{4}\%$ in the test range.

C. Total Pressure Survey System

The total pressure survey system was designed to utilize the same test stations as the skin-friction balance. The system consisted of the total pressure sensing element and the drive mechanism.

1. Total pressure sensing element

Two different total pressure probe designs were used in the tests; one for the flat-plate tests and the other for the diffuser floor tests. The thinner boundary layers on the flat-plate model permitted the use of a single-tube probe with a double-wedge support. A four-tube rake with a stronger support was used for the diffuser floor tests because of the thicker boundary layers and resulting large air loads. The stronger support had a rectangular cross section with a wedge-shaped leading edge. Vertical separation between the four tubes on the rake was 1.5 in. Three of the prongs on the rake were constructed of 0.064-in.-o.d. stainless-steel tubing; the lower prong had an 0.042-in. o.d. as did the single-tube probe used in the flat-plate tests. For both elements in the down position, the tube in contact with the test surface was configured such that it was spring loaded against the surface. This provision permitted the tube tip to remain on the surface during the initial movement of the traversing element so that the tube position at the instant the tube left the wall could be determined by observation of a change in the total pressure reading. The tube sizes and separation on the rake were consistent with data of Refs. 2–4 in regard to interference effects.

2. Drive mechanism

The pressure sensing element was connected to the electrically powered drive mechanism, which was attached to the underside of the test surface. The linkage of the system was such that the pressure sensing element could be extended from the wall to a position $1\frac{1}{2}$ in. into the flow over the plate. The movement of the element was continuous, but it moved slower near the wall than at the other end of the travel. A complete traverse required approximately 7 sec. It was determined that the response of the pressure recording system was sufficiently fast so that any error introduced by the continuous motion would be negligible.

D. Flat-Plate Model

The flat-plate model used in the first phase of the test program was 10 ft long and completely spanned the 4-ft width

of the tunnel test section. The installation of the plate in the tunnel test section is shown schematically in Fig. 1. The edges of the plate along the sidewalls were sealed to prevent flow from the lower to the upper test surface. Provisions were made for two balance-survey stations; one 3 ft and the other 9 ft aft of the leading edge along the plate centerline.

There were 34 static pressure taps, 32 of which were located along the centerline of the plate and connected to the same transducer through a scanivalve. A static pressure tap was located just forward and slightly off center of each of the two measuring stations. These two taps were connected to separate transducers, so that each data sampling would include the static pressure at the measuring stations. Cycling of the scanivalve required approximately 3 sec.

The finish required for an aerodynamically smooth surface was determined, using the method of Ref. 5, to be 100 μin. To be conservative, a finer finish was specified for the plate, and after fabrication had been completed the mean surface finish was measured and found to be 10 μin.

For the low-unit Reynolds number tests (8×10^6/ft) a boundary-layer trip was used to minimize the extent of laminar flow near the leading edge. It was determined from the data of Refs. 6 and 7 that a 0.012-in.-diam wire bonded to the plate $\frac{1}{2}$ in. from the leading edge would be sufficient to trip the boundary layer at this point with a negligible increase in momentum thickness. For the other tests, with unit Reynolds number above 15×10^6, the wire trip was removed. It was estimated that for these tests the maximum error in the x dimension of the effective leading edge for the turbulent boundary layer, and consequently the Reynolds number, was 5%. A 5% variation in the Reynolds number represents approximately a 1% change in the skin-friction coefficient, and, therefore, this accuracy was considered satisfactory. Consistent with the data of Ref. 8, the leading edge thickness of the plate was held to from 0.002 to 0.004 in. in order to minimize the bluntness effects.

E. Diffuser Floor Test Surfaces

The variable area supersonic diffuser of the LTV High-Speed Tunnel was used in the open position, and fairing modifications were made to the ceiling and floor. This in effect provided a long extension to the tunnel test section. Three balance-survey stations were provided in the floor fairing which consisted of three plates of $\frac{5}{8}$-in.-thick, 48-in.-wide, rolled aluminum stock. The fairing on the diffuser ceiling was of the same material, but was not instrumented. The plates were attached to the diffuser walls by machine screws with the heads countersunk into the surface exposed to the flow. All gaps and holes were sealed and filled to obtain a smooth surface. The surface finish of the stock plates was approximately 25 μin., which was well within the requirements for an aerodynamically smooth surface under the flow conditions of the tests.

As with the flat-plate model, 34 static pressure taps were provided along the floor with a nominal spacing of 1 ft. These taps were connected to a transducer through a scanivalve and some of these taps, from which continuous readings were desired, were also connected to separate transducers.

A schematic of the installation is shown in Fig. 1. Although both the flat-plate installation and the diffuser floor test surfaces are illustrated in this drawing, they were not tested simultaneously.

F. Test Procedure

The procedure followed in conducting both tests was basically the same. Preinstallation calibrations were made of the skin-friction balance, the survey system position indicator, and the pressure transducers. After installation of the test surface and the associated instrumentation had been completed, additional check calibrations were performed to insure all systems were functioning properly. A check calibration of the skin-friction balance was made before each run during which balance measurements were made. Complete calibrations of the balance and survey system position were made at the beginning and end of the runs at each test station.

Two skin-friction balances were available for the flat-plate tests and simultaneous measurements were obtained at both stations. Total pressure surveys were made at the back station only on the flat-plate model. Only one balance was available for the diffuser floor tests. The test configurations were arranged so that balance and total pressure survey data were obtained at each diffuser test station for the selected tunnel stilling chamber pressure conditions.

III. Data Reduction and Analysis

The data reduction procedure described in the following paragraphs involves only the calculations required to convert the pressure and shear stress data to the form of the various boundary-layer parameters. Conversion of the recorded data to pressure and shear stress data was accomplished by the LTV Wind-Tunnel Laboratories personnel. Extensive use was made of the IBM 7090 digital computer in both parts of the data reduction calculations.

A. External Flow Conditions

The Mach number at the outer edge of the boundary layer at any given test location can be determined by any one of the following three relationships:

$$\frac{P_1}{P_0} = \left(1 + \frac{\gamma - 1}{2} M_1^2\right)^{-\gamma/(\gamma-1)} \tag{1}$$

$$\frac{P_{t_2}}{P_0} = \left[\frac{(\gamma + 1)M_1^2}{(\gamma - 1)M_1^2 + 2}\right]^{\gamma/(\gamma-1)} \times \left[\frac{\gamma + 1}{2\gamma M_1^2 - (\gamma - 1)}\right]^{\gamma/(\gamma-1)} \tag{2}$$

$$\frac{P_{t_2}}{P_1} = \left[\frac{(\gamma + 1)M_1^2}{2}\right]^{\gamma/(\gamma-1)} \left[\frac{\gamma + 1}{2\gamma M_1^2 - (\gamma - 1)}\right]^{1/(\gamma-1)} \tag{3}$$

Equations (1) and (2) require isentropic flow from the stilling chamber to the point in question. Equations (2) and (3) assume a normal shock in front of an impact pressure probe. According to the thin boundary-layer concept, the static pressure was assumed to be constant across the boundary layer; therefore, Eqs. (1) and (3) can be used with P_1 measurements made at the wall. The Rayleigh pitot formula, Eq. (3), was used for the determination of M_1 for the tests in which impact pressure probe data were available at a given station. At the forward station on the flat-plate model, only static pressure data were available, and so Eq. (1) was used to determine M_1.

The other property required to establish the thermodynamic state was the static temperature. This was determined from

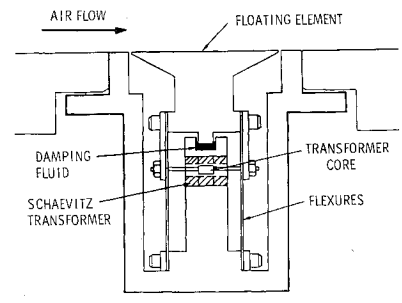

Fig. 2 Schematic drawing of floating element skin-friction balance.

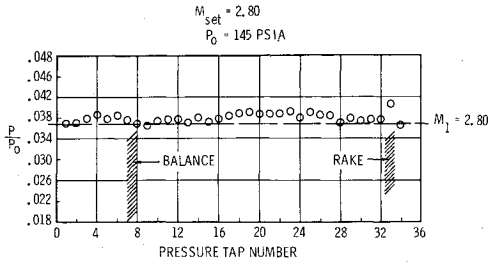

Fig. 3 Static pressure distribution along the flat-plate model.

the following relationship using the measured stilling chamber temperature and M_1 as determined in the manner just discussed:

$$T_1/T_0 = \{1 + [(\gamma - 1)/2]M_1^2\}^{-1} \quad (4)$$

The density ρ_1 was then determined from the ideal gas equation of state

$$\rho_1 = p_1/RT_1 \quad (5)$$

The external flow dynamic pressure was calculated by

$$q_1 = (\gamma/2)P_1M_1^2 \quad (6)$$

or

$$q_1 = \rho_1U_1^2/2 \quad (7)$$

where

$$U_1 = M_1(\gamma RT_1)^{1/2} \quad (8)$$

The unit Reynolds number is defined as

$$R/\text{ft} = \rho_1U_1/\mu_1 \quad (9)$$

where the coefficient of viscosity was calculated by a form of the Sutherland equation:

$$\mu(T) = 6.08 \times 10^{-7}[1216/(T + 216)](T/1000)^{3/2} \quad (10)$$

B. Momentum Thickness

The momentum thickness, which is an indication of the momentum deficit in the boundary layer, is defined as

$$\theta = \int_0^\delta \frac{\rho U}{\rho_1 U_1}\left(1 - \frac{U}{U_1}\right) dy \quad (11)$$

The integrand was evaluated at each point sampled in the boundary-layer total pressure survey. The local Mach number M was determined from Eq. (3), and the velocity ratio by

$$U/U_1 = (M/M_1)(T/T_1)^{1/2} \quad (12)$$

where the temperature ratio at any point in the boundary layer was determined from

$$\frac{T}{T_1} = \left[\frac{1 + [(\gamma - 1)/2]M_1^2}{1 + [(\gamma - 1)/2]M^2}\right] \quad (13)$$

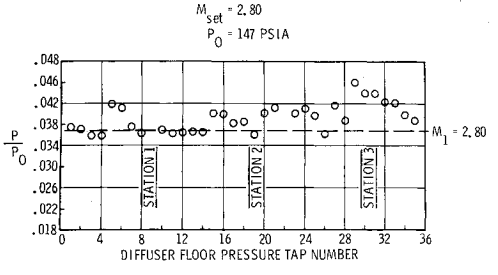

Fig. 4 Static pressure distribution on the diffuser floor.

Equation (13) is based on the assumption of isoenergetic flow across the boundary layer. This assumption has been shown to provide a satisfactory approximation for the adiabatic wall case. Since the static pressure has been assumed to be constant across the boundary layer, the density ratio can be expressed as

$$\rho/\rho_1 = T_1/T \quad (14)$$

The integration required for the evaluation of the momentum thickness was accomplished numerically by the trapezoidal rule. The boundary-layer displacement thickness defined as

$$\delta^* = \int_0^\delta \left(1 - \frac{\rho U}{\rho_1 U_1}\right) dy \quad (15)$$

was also evaluated in the same manner as θ.

C. Matching Procedure

Two separate runs were required to obtain the shear-stress measurement and the total pressure survey data at any given test station for a desired unit Reynolds number. The Mach number was held constant between any two runs, but small variations in P_0 could not be avoided. Stilling chamber temperature could not be accurately controlled, and in some cases there were significant differences between the measured temperatures of the two runs which had to be matched. These pressure and temperature differences generally resulted in small but not negligible differences in the unit Reynolds number R/ft between the two runs. The local skin-friction coefficient, defined as

$$C_f = \frac{\tau_w}{\rho_1 U_1^2/2} = \frac{\tau_w}{q_1} \quad (16)$$

varies with Reynolds number only for any given Mach number. It was therefore necessary to correct the shear-stress measurements for the variation in unit Reynolds number. This was accomplished by plotting C_f vs R/ft for each test station, then determining from the curve the value of C_f corresponding to the R/ft of the total pressure survey runs. The maximum correction of C_f by this procedure was 1.6% with most of the data being corrected by less than 1%.

D. Effective Origin of the Boundary Layer

For the diffuser floor tests, the distance x from the origin of the boundary layer to the measuring station cannot be physically measured. In order to compare the skin-friction data obtained with the theoretical C_f-R_x relationships, it was necessary to determine the effective origin of the boundary layer. This was accomplished in the following manner. Following the analysis of Wilson,[2] a relationship between the local skin-friction coefficient and the momentum thickness Reynolds number R_θ was determined by using the law of the wall velocity distribution in Eq. (11) to obtain the following expression:

$$[\sin^{-1}(\sigma)^{1/2}]\left[\left(\frac{T_1}{T_w}\right)\left(\frac{1}{\sigma}\right)\left(\frac{1}{C_f}\right)\right]^{1/2} = 4.15 \log_{10}\left(R_\theta \frac{\mu_1}{\mu_w}\right) + 2.78 \quad (17)$$

The validity of this relationship for the present test conditions has been established by comparison with the experimental data obtained. Equation (17) was rewritten in the form

$$C_f = \alpha^2/(\ln R_\theta + \beta)^2 \quad (18)$$

Table 1 Summary of results of diffuser floor tests

Sta.	M_1	T_0, °R	θ, in.	δ^*, in.	δ, in.	R_θ	R_X	C_f
1	2.831	536	0.1915	0.8942	4.0985	4.24×10^5	8.27×10^8	0.000900
1	2.843	525	0.1774	0.8449	4.6062	3.26×10^5	6.11×10^8	0.000953
1	2.865	531	0.1974	0.9437	4.2878	2.12×10^5	3.76×10^8	0.000987
1	2.897	520	0.2289	1.1083	4.5105	1.82×10^5	3.18×10^8	0.001020
2	2.787	568	0.2676	1.2118	5.4807	5.57×10^5	1.12×10^9	0.000849
2	2.809	570	0.2663	1.2217	5.6825	4.46×10^5	8.73×10^8	0.000874
2	2.828	564	0.2770	1.2862	5.5314	2.79×10^5	5.12×10^8	0.000946
3	2.669	548	0.3195	1.3650	6.0471	7.02×10^5	1.41×10^9	0.000862
3	2.693	541	0.3276	1.4195	6.2713	5.95×10^5	1.18×10^9	0.000891

where

$$\alpha = [\sin^{-1}(\sigma)^{1/2}]\left[\left(\frac{T_1}{T_w}\right)\left(\frac{1}{\sigma}\right)\right]^{1/2}\frac{1}{4.15\log_{10}e} \quad (19)$$

$$\beta = \ln(\mu_1/\mu_w) + (2.78/4.15\log_{10}e) \quad (20)$$

The local skin-friction coefficient for the zero pressure gradient case may also be expressed as

$$C_f = 2(d\theta/dx) = 2(dR_\theta/dR_x) \quad (21)$$

according to momentum theory. The combination of Eqs. (18) and (21) results in the differential equation

$$(\alpha^2/2)dR_x = [(\ln R_\theta + \beta)^2]dR_\theta \quad (22)$$

A solution of Eq. (22) was found to be

$$R_x = (2/\alpha^2)\{R_\theta[(\ln R_\theta - 1)^2 + 2\beta(\ln R_\theta - 1) + \beta^2 + 1] + C\} \quad (23)$$

where C is the constant of integration. Evaluation of Eq. (23) for the flat-plate data obtained in the present tests indicated that

$$C = 4.96 \times 10^5$$

Note that Eq. (23) was established on the basis of α and β being constant. Since α and β are functions of M_1, the constant C must also be considered as being some unknown function of M_1 until data at other Mach numbers are available. Equation (23) was used to determine the effective R_x for the diffuser floor skin-friction measurements.

E. Boundary-Layer Thickness

The boundary-layer thickness δ was determined by a method recommended by Coles in Ref. 9. The term $(1 - u/u_1)^{2/3}$ was evaluated for the data obtained in the outer portion of the boundary layer, and this term was then graphed with respect to y. The y intercept of a straight line curve fit of the data in this form was taken as the boundary-layer thickness δ.

IV. Discussion of Results

The results of primary importance obtained from the present tests are the skin-friction data; the velocity profile data are of a secondary or supporting nature. A summary of the results obtained in the diffuser floor tests are presented in Table 1. Also of a supporting nature are the pressure distribution data for the flat-plate model and the diffuser floor. Typical pressure distributions along these surfaces at the test Mach number are presented in Figs. 3 and 4. These distributions are considered acceptable and consistent with other experimental results on similar surfaces. The velocity profile data, as discussed in the following paragraphs, indicated that any disturbances and nonisobaric conditions along the surfaces had negligible effect upon the boundary-layer characteristics.

A. Velocity Profile Data

It has been well established experimentally that turbulent boundary layers in both subsonic and supersonic flows exhibit certain velocity similarity characteristics over the complete Reynolds number range of experimentally studied turbulent flows. These universal similarity characteristics are illustrated by two different velocity profile laws: the law of the wall and the velocity defect law. The law of the wall velocity profile can be derived from mixing-length theory, and as the name implies, this law is valid in the region of the boundary layer near the wall. Wall effects such as surface roughness and heat transfer are reflected in the law of the wall profiles, but external flow effects are not apparent in these profiles. The law of the wall variables are

$$\phi = U/U_\tau \qquad \eta = \rho_w U_\tau y/\mu_w$$

where

$$U_\tau = (\tau_w/\rho_w)^{1/2}$$

For compressible flows, the nondimensional velocity variable ϕ must be corrected for the compressibility effects so that

$$\phi^* = [\phi_1/(\sigma)^{1/2}]\sin^{-1}[(\sigma)^{1/2}(\phi/\phi_1)]$$

Law of the wall velocity profiles for a typical run on the flat-plate model and on the diffuser floor are presented in Figs. 5 and 6, respectively. The experimental data are compared with tabulated values of Coles.[9] It may be noted that there is excellent agreement in both cases between the experimental data and Coles' law of the wall, as with all of the law of the wall profile data obtained in the present test series. The agreement of the present data with Coles' tabulated values in the region of expected validity indicates that the data are consistent with other turbulent boundary-layer data; the good agreement also signifies that the mixing-length concept provides a valid method of analysis for the very high Reynolds number range of the present tests.

The velocity defect law has been shown to correlate all turbulent, zero pressure gradient boundary-layer data, and does not reflect any of the wall effects but is sensitive to

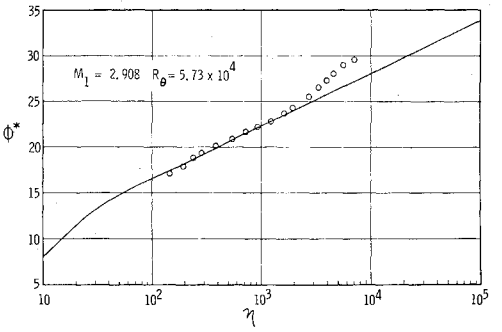

Fig. 5 Typical law of the wall velocity profile on the flat-plate model.

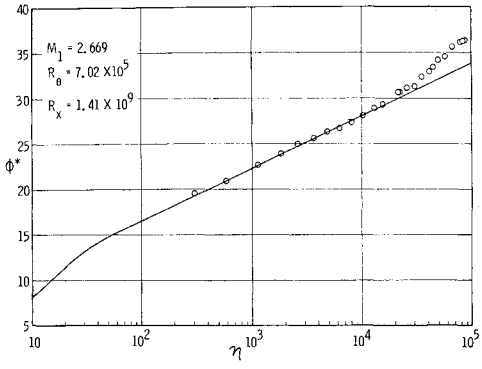

Fig. 6 Typical diffuser floor law of the wall velocity profile.

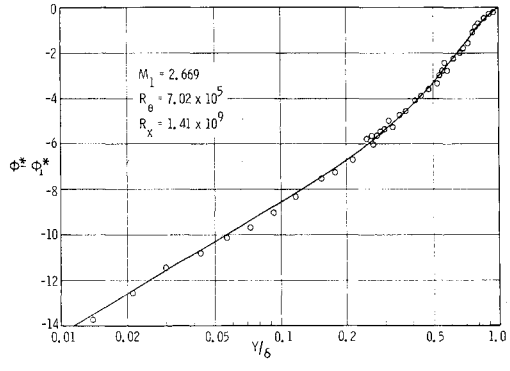

Fig. 8 Typical diffuser floor velocity defect law.

external flow effects. The velocity defect law relates the nondimensional velocity difference

$$\phi^* - \phi_1^*$$

to the ratio y/δ. This functional relationship also has been tabulated by Coles.[9] The boundary-layer thickness δ was defined as discussed in the previous section. Typical velocity defect law profiles obtained in the present tests are presented in Figs. 7 and 8 for the flat-plate model and diffuser floor, respectively. The good agreement between the data obtained in these tests and Coles' tabulated values is an indication that the boundary layers investigated satisfied the condition of zero pressure gradient equilibrium as discussed by Clauser.[10] The good agreement is also indicative of the fact that the disturbances in the flow along the test surfaces have a negligible effect on the boundary-layer characteristics. Therefore, the boundary layers being investigated can for all practical purposes be considered as isobaric, and the zero pressure gradient momentum equation can then be used to determine the effective origin of the boundary layer.

B. Variation of Skin-Friction with Reynolds Number

Figure 9 presents the variations of local skin-friction coefficient with the momentum thickness Reynolds number. The present data are compared with a theoretical relationship [Eq. (17)], which was derived following the analysis of Wilson.[2] The constant term 2.78 was evaluated from available incompressible experimental data in a manner consistent with the rest of the Wilson analysis. The term containing the viscosity ratio has been retained in this form, whereas Wilson made the substitution

$$\mu_1/\mu_w = (T_1/T_w)^{0.768}$$

The theoretical curve of Fig. 9 is for the nominal flow conditions of the test, $M_1 = 2.80$ and $T_w/T_1 = 2.395$. The agreement between the present experimental data and the theory is very good. Of particular significance is that the data of the two different tests are in such good agreement with each other and establish a definite trend with no discontinuity. The validation of Eq. (17) for the test conditions permitted its use in the determination of the effective origin of the boundary layer as discussed previously. Had the experimental data not verified Eq. (17) it would have been necessary to establish, probably by empirical means, the functional relationship between C_f and R_θ in order to determine the effective origin. It is noted that the determination of x for the diffuser floor data involves the integration of Eq. (17). Using the experimental data obtained in the flat-plate tests to determine the constant of integration, rather than the usual boundary conditions of $\theta = 0$ at $x = 0$, permitted the integration over a range of known validity. The validity of Eq. (17) for all values of θ has not been established and it is expected that it would not be valid near the $\theta = 0$ condition.

The variation of the local skin-friction coefficient C_f with respect to the Reynolds number based on the length x is presented in Fig. 10. The present data are again compared with the theory of Wilson for the nominal flow conditions of the test. It may be observed that the agreement between theory and experiment, in this case too, is good. There were sufficient data obtained in the flat-plate tests to provide an adequate repeatability check of the shear stress measurements. It may be noted from Fig. 10 that the maximum deviation from a mean value is of the order of $\pm 2\%$. The most significant confirmation of the accuracy of the data is illustrated by the excellent agreement between data obtained at different stations on the flat plate, but each at approximately the Reynolds number of $R_x = 7 \times 10^7$.

It may be noted in Fig. 10 that the two datum points obtained at the aftmost diffuser station (station 3) have the greatest deviation from the theory, but also these two points have the greatest deviation from the nominal flow conditions.

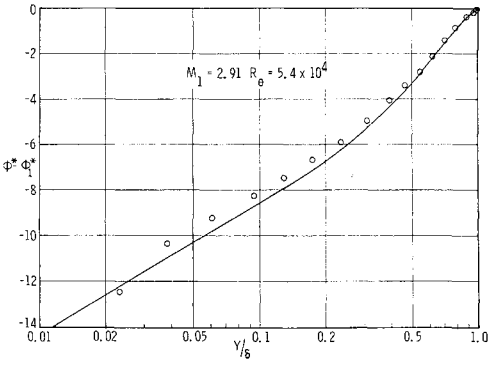

Fig. 7 Typical velocity defect law for the flat-plate model.

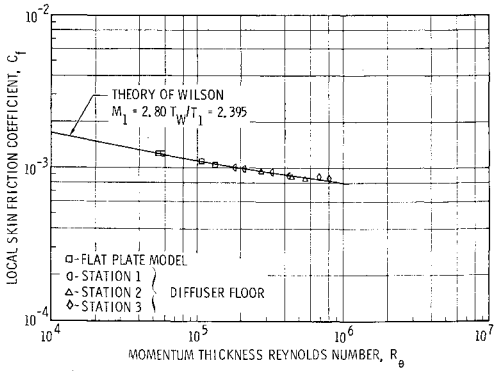

Fig. 9 Variation of local skin-friction coefficient with momentum thickness Reynolds number.

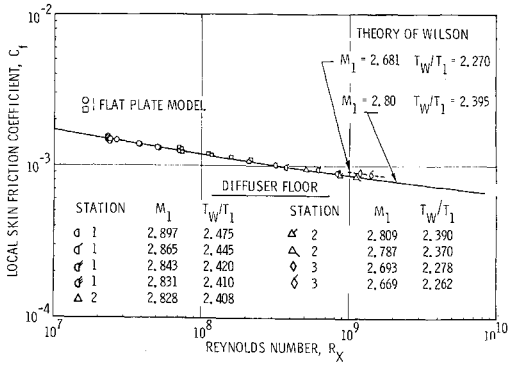

Fig. 10 Variation of local skin-friction coefficient with Reynolds numbers.

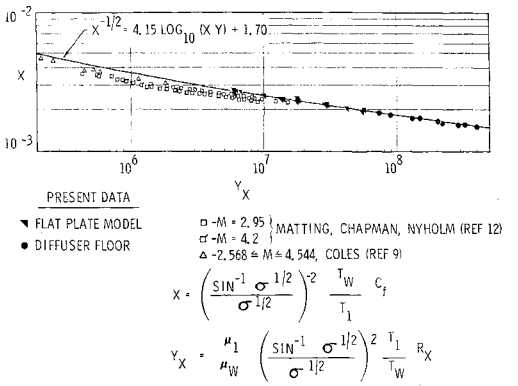

Fig. 12 Comparison of experimental data on a generalized basis to the C_f-R_x theory of Wilson.

Theoretical values of C_f based on average conditions for the diffuser station 3 points are illustrated by the dashed line in Fig. 10. It may be observed that the agreement between experiment and theory for these average flow conditions appears to be quite good.

Wilson's skin-friction relationships can be expressed in generalized forms so that data for different Mach numbers and temperatures can be compared graphically to a single theoretical curve. The comparison of the present data to the generalized Wilson $C_f - R_\theta$ relation may be seen in Fig. 11, and the comparison to the generalized $C_f - R_x$ equation is presented in Fig. 12. Experimental data from other sources[3, 9, 11, 12] for flat plate, adiabatic wall, supersonic flows are also illustrated in these two figures. A representative sample of the incompressible data presented in Ref. 13 is also shown in Fig. 11. All of these other skin-friction data were obtained by direct measurements using floating-element-type balances similar to that used in the present tests. These results are presented as published, and no attempt has been made to normalize these data in regard to the method of determining the effective origin of the turbulent boundary layer. The data of Ref. 12 were also obtained on the floor of a tunnel and the effective length x was measured from experimentally determined points corresponding to the end of transition from laminar to turbulent flow.

In some cases, the data from these other sources were incomplete in that only nominal values of flow conditions, such as Mach number and total temperature, were known. The experimental data presented in Figs. 11 and 12 represent a range of flow conditions of

$$0.15 \leqq M_1 \leqq 4.544$$

$$8.32 \times 10^3 \leqq R_\theta \leqq 7.02 \times 10^5$$

$$2.81 \times 10^6 \leqq R_x \leqq 1.41 \times 10^9$$

It may be observed that agreement between the experimental data and Wilson's theories is generally good. It is also noted that the Wilson theory is slightly conservative in the Reynolds number range where the bulk, and consequently the greater scatter, of the data appear. Therefore, it can be concluded that the Wilson theory would be satisfactory for predicting skin-friction drag design loads.

Figure 13 presents a comparison between the C_f-R_x theories of Wilson, Van Driest,[14] and a reference temperature method using the Schultz-Grunow expression for the constant property (incompressible flow) relationship. This comparison is made for the nominal flow conditions of this test at $M = 2.8$ and $T_0 = 100°\text{F}$. It may be noted that there is virtually no difference between the Wilson and Van Driest methods, whereas the Schultz-Grunow reference temperature method predicts values of C_f approximately 10 to 15% lower. A recent survey of a large amount of available experimental turbulent boundary-layer data[15] indicated that the Van Driest and Wilson theories appeared to have the best over-all agreement of the generally known theories.

V. Conclusions

Experimental boundary-layer investigations have been accomplished on a flat-plate model, 4 ft wide by 10 ft long, and on the open diffuser wall in a blow-down tunnel at a nominal Mach number of 2.8. Local shear stress measurements were made as well as total pressure surveys through the boundary layer. Reynolds numbers from 2.32×10^7 to 1.41×10^9 were obtained which represent a considerable extension to existing experimental data.

The resulting velocity profiles were consistent and correlate well with lower Reynolds number data. Of significance is the fact that the velocity profiles on the diffuser wall indicated an equilibrium condition for the zero pressure gradient case. This condition permitted integration of the zero pressure gradient momentum equation to obtain an equivalent flat plate length Reynolds number.

The skin-friction data are also consistent and correlate well with lower Reynolds number data. Of most significance

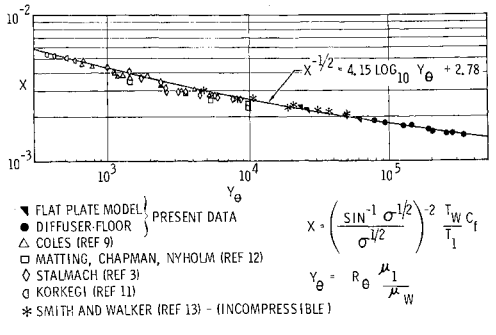

Fig. 11 Comparison of experimental data on a generalized basis with C_f-R_θ theory of Wilson.

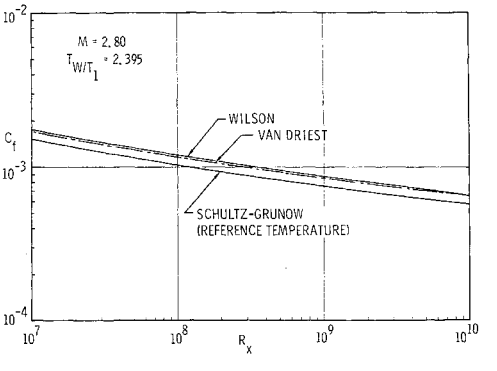

Fig. 13 Comparison of local skin-friction theories.

is the fact that the data on the flat plate and on the diffuser wall are consistent and lie along a continuous curve. The data agree extremely well with the analysis of Wilson,[2] and it is concluded that this analysis can be used with confidence over the range of the experimental data.

References

[1] "High speed wind tunnel handbook," High-Speed Wind Tunnel Staff, Chance Vought Corp. Rept. AER-E1R-13552 (September 1962).

[2] Wilson, R. E., "Turbulent boundary layer characteristics at supersonic speed—Theory and experiment," J. Aeronaut. Sci. **17**, 585–594 (1950).

[3] Stalmach, C. J., "Experimental investigation of the surface impact pressure probe method of measuring local skin friction at supersonic speeds," Rept. DRL-410, CF-2675, Defense Research Lab., Univ. of Texas, Austin, Texas (January 1958).

[4] Lacy, J. R., "Interference effects between total-pressure probes in the boundary layer of a supersonic wind tunnel," Rept. DRL-420, Defense Research Lab., Univ. of Texas, Austin, Texas (January 1958).

[5] Fenter, F. W., "The turbulent boundary layer on uniformly rough surfaces at supersonic speeds," Rept. RE-E9R-2, Vought Research Center, Chance Vought Aircraft, Inc., Dallas, Texas (December 1959).

[6] Van Driest, E. R. and Blumer, C. B., "Effect of roughness on transition in supersonic flow," Air Force Office of Scientific Research AFOSR TN60-1164, North American Aviation, Inc., Downey, Calif. (March 1960).

[7] Luther, M., "Fixing boundary-layer transition on supersonic-wind tunnel models," Rept. 20-256, Jet Propulsion Lab., California Institute of Technology, Pasadena, Calif. (August 1955).

[8] Brinish, P. F. and Sands, N., "Effect of bluntness on transition for a cone and a hollow cylinder at Mach 3.1," NACA TN 3979 (1957).

[9] Coles, D., "Measurements in the boundary layer on a smooth flat plate in supersonic flow," Ph.D. Thesis, Guggenheim Aeronautical Lab., California Institute of Technology, Pasadena, Calif. (1953).

[10] Clauser, F. H., "The behavior of turbulent boundary layers," *Second Symposium on Aerodynamics* (University of Toronto Press, Toronto, Canada, February 1954).

[11] Korkegi, R. H., "Transition studies and skin friction measurements on an insulated flat plate at a hypersonic Mach number," Memo. 17, Guggenheim Aeronautical Lab., California Institute of Technology, Pasadena, Calif. (July 1964).

[12] Matting, F. W., Chapman, D. R., Nyholm, J. R., and Thomas, A. G., "Turbulent skin friction at high Mach numbers and Reynolds numbers in air and helium," NASA TR R-82 (1960).

[13] Smith, D. W. and Walker, J. H., "Skin friction measurements in incompressible flow," NASA TR R-26 (1959).

[14] Van Driest, E. R., "The turbulent boundary layer with variable Prandtl number," Rept. AL-1914, North American Aviation, Inc., Downey, Calif. (April 1954).

[15] Spalding, D. B. and Chi, S. W., "Skin friction exerted by a compressible fluid stream on a flat plate," AIAA J. **1**, 2160–2161 (1963).